of $CrH^+ + R$,[30] such that the surfaces leading to these two product channels must cross. This difference in energetics is illustrated by the observation that cross sections for $CrH + R^+$ are higher than those for $CrH^+ + R$ at thermal energies (Tables II–V), the opposite of the results obtained at higher kinetic energies.

A second detail concerns the alkane elimination reactions mentioned in the mechanism section above. For demethanation in the methylpropane and butane systems, the ionic species formed in the reactions of $Cr^+(^6S)$ have the $Cr^+{=}C(CH_3)_2$ and $Cr^+{=}CHCH_2CH_3$ structures.[15] The $Cr{=}C$ double bond demands that these species have quartet spin ground states, as has been calculated for $Cr^+{=}CH_2$.[31,32] Since the CH_4 product is $^1A_1$, formation of these products from $Cr^+(^6S)$ is spin-forbidden. This explicitly demonstrates that the reactions of the $Cr^+(^6S)$ ground state with alkanes must involve a coupling of sextet and quartet surfaces. This coupling presumably occurs during the C–C bond activation step that forms intermediate I and its analogues. In contrast, the ionic species formed in the reactions of excited-state Cr^+ with methylpropane and butane presumably have the chromium ion–propene structure. Since the ground state of this species must be formed from a dative interaction of ground-state $Cr^+(^6S)$ with propene, it should have sextet spin. However, excited states of $Cr(C_3H_6)^+$ can be formed by the interaction of propene with the other states of Cr^+. As long as the $Cr^+(^4D, {}^4G)$–propene bond energy exceeds the energy required to remove methane from the alkanes (19 and 17 kcal/mol in the methylpropane and butane cases, respectively), as seems reasonable, reaction of the excited quartet states of Cr^+ with these alkanes to form excited states of $Cr(C_3H_6)^+$ can still be exothermic.

Acknowledgment. This work was supported by the National Science Foundation under Grant No. CHE-8917980.

Registry No. Cr^+, 14067-03-9; propane, 74-98-6; butane, 106-97-8; methylpropane, 75-28-5; dimethylpropane, 14067-03-9.

---

(30) This is based on an ionization energy for CrH of ~7.6 eV derived from $D°(Cr^+–H) = 32.5 \pm 1.8$ kcal/mol[12] and $D°(Cr–H) = 53 \pm 4$ kcal/mol (Chen, Y.-M.; Clemmer, D. E.; Armentrout, P. B. Work in progress).

(31) Alvarado-Swaisgood, A. E.; Allison, J.; Harrison, J. F. *J. Phys. Chem.* **1985**, *89*, 2517.

(32) Carter, E. A.; Goddard, W. A. *J. Phys. Chem.* **1984**, *88*, 1485.

An ab Initio MO/SD-CI Study of Model Complexes of Intermediates in Electrochemical Reduction of CO_2 Catalyzed by $NiCl_2$(cyclam)

Shigeyoshi Sakaki

Contribution from the Department of Applied Chemistry, Faculty of Engineering, Kumamoto University, Kurokami, Kumamoto 860, Japan. *Received April 5, 1991*

Abstract: Ab initio MO/SD-CI calculations of several Ni^I– and Ni^{II}–CO_2 complexes indicate that CO_2 can coordinate to $Ni^IF(NH_3)_4$, yielding a stable η^1-CO_2 complex, but cannot to $[Ni^{II}F(NH_3)_4]^+$, $[Ni^I(NH_3)_4]^+$, and $[Ni^I(NH_3)_5]^+$. The HOMO of $Ni^IF(NH_3)_4(\eta^1\text{-}CO_2)$ is largely contributed from the O p_π orbital and lies higher in energy than the HOMO (nonbonding π orbital) of the uncomplexed CO_2. At the same time, the electron density increases around the O atom upon CO_2 coordination. As a result, the coordinated CO_2 in $Ni^IF(NH_3)_4(\eta^1\text{-}CO_2)$ is activated to electrophilic attack and is expected to undergo facile protonation. MO calculations show that the second one-electron reduction can easily occur in the protonated species $[NiF(NH_3)_4(CO_2H)]^+$, yielding the triplet state of $[NiF(NH_3)_4(CO_2H)]$, but cannot in the unprotonated species $NiF(NH_3)_4(CO_2)$. The second reduction significantly weakens the C–OH bond, which suggests that OH^- easily dissociates from $[NiF(NH_3)_4(CO_2H)]$, yielding the triplet state of $[Ni^{II}F(NH_3)_4(CO)]^+$. The CO coordinate bond to Ni^{II} is calculated to be weak, which suggests that CO easily dissociates from Ni^{II}. All these results support Sauvage's reaction mechanism of electrocatalytic reduction of CO_2 by $NiCl_2$(cyclam).

Introduction

CO_2 conversion into useful substances is of great interest for a variety of reasons including a resource utilization problem.[1] Of many attempts of CO_2 conversion, electrochemical[2-15] and photochemical[16-20] reduction of CO_2 catalyzed by transition-metal complexes have been actively investigated. In those reactions,

---

(1) For instance (a) Collin, J.-P.; Sauvage, J.-P. *Coord. Chem. Rev.* **1989**, *93*, 245. (b) Behr, A. *Angew. Chem., Int. Ed. Engl.* **1988**, *27*, 661. (c) Culter, A. R.; Hanna, P. K.; Vites, J. C. *Chem. Rev.* **1988**, *88*, 1363. (d) Braunstein, P.; Matt, D.; Nobel, D. *Chem. Rev.* **1988**, *88*, 747. (e) Walther, D. *Coord. Chem. Rev.* **1987**, *79*, 135. (f) Darensbourg, D. J.; Kudaroski, R. A. *Adv. Organomet. Chem.* **1983**, *22*, 129. (g) Palmer, D. A.; Van Eldik, P. *Chem. Rev.* **1983**, *83*, 651. (h) Sneeden, R. P. A.; Villeurbanne, C. N. R. S. In *Comprehensive Organometallic Chemistry*; Wilkinson, G., Ed.; Pergamon Press: Oxford, 1982; p 225.

(2) Meshitsuka, S.; Ichikawa, M.; Tamaru, K. *J. Chem. Soc., Chem. Commun.* **1974**, 158.

(3) (a) Hiratsuka, K.; Takahashi, K.; Sasaki, H.; Toshima, S. *Chem. Lett.* **1977**, 1137. (b) Takahashi, K.; Hiratsuka, K.; Sasaki, H.; Toshima, S. *Chem. Lett.* **1979**, 305.

(4) Fisher, B.; Eisenberg, R. *J. Am. Chem. Soc.* **1980**, *102*, 7363.

(5) Tezuka, M.; Yajima, T.; Tsuchiya, A.; Matsumoto, Y.; Uchida, Y.; Hidai, M. *J. Am. Chem. Soc.* **1982**, *104*, 6834.

(6) (a) Beley, M.; Collin, J.-P.; Ruppert, R.; Sauvage, J.-P. *J. Chem. Soc., Chem. Commun.* **1984**, 1315. (b) Beley, M.; Collin, J.-P.; Ruppert, R.; Sauvage, J.-P. *J. Am. Chem. Soc.* **1986**, *108*, 7461.

(7) Kapusta, S.; Hackerman, N. *J. Electrochem. Soc.* **1984**, *131*, 1511.

(8) Lieber, C. M.; Lewis, N. S. *J. Am. Chem. Soc.* **1984**, *106*, 5033.

(9) Slater, S.; Wagenknecht, J. H. *J. Am. Chem. Soc.* **1984**, *106*, 5367.

(10) (a) Bolinger, C. M.; Sullivan, B. P.; Conrad, K.; Gilbert, J. A.; Story, N.; Meyer, T. J. *J. Chem. Soc., Chem. Commun.* **1985**, 796. (b) O'Toole, T. R.; Margerum, L. D.; Westmoreland, T. D.; Vining, W. J.; Murray, R. W.; Meyer, T. J. *J. Chem. Soc., Chem. Commun.* **1985**, 1416.

(11) Daniele, S.; Ugo, P.; Bontempelli, G.; Florani, M. *J. Electroanal. Chem. Interfacial Electrochem.* **1987**, *219*, 259.

(12) (a) Ishida, H.; Tanaka, H.; Tanaka, K.; Tanaka, T. *Chem. Lett.* **1987**, 597. (b) Ishida, H.; Tanaka, H.; Tanaka, K.; Tanaka, T. *J. Chem. Soc., Chem. Commun.* **1987**, 131.

(13) Christensen, P. A.; Hamnett, A.; Muir, A. V. G. *J. Electroanal. Chem. Interfacial Electrochem.* **1988**, *241*, 361.

(14) Bruce, M. R. M.; Megehee, E.; Sullivan, B. P.; Thorp, H.; O'Toole, T. R.; Downard, A.; Meyer, T. J. *Organometallics* **1988**, *7*, 238.

(15) Hurrell, H. C.; Mogstad, A.-L.; Usifer, D. A.; Potts, K. T.; Abruna, H. D. *Inorg. Chem.* **1989**, *28*, 1080.

(16) Hawecker, J.; Lehn, J.-M.; Ziessel, R. *J. Chem. Soc., Chem. Commun.* **1983**, 56.

(17) (a) Willner, I.; Mandler, D.; Riklin, A. *J. Chem. Soc., Chem. Commun.* **1986**, 1022. (b) Belmore, K. A.; Vanderpool, R. A.; Tsai, J.-C.; Khan, M. A.; Nicholas, K. M. *J. Am. Chem. Soc.* **1988**, *110*, 2004.

0002-7863/92/1514-2055$03.00/0

transition-metal complexes are used, in expecting that an inert CO_2 molecule is activated by coordination to transition metals and is easily converted to useful substances. One of the good examples is the electrochemical reduction of CO_2 catalyzed by $NiCl_2$(cyclam).[4,6] The reaction mechanism has been proposed by Sauvage et al.;[6b] $NiCl_2$(cyclam) is electrochemically reduced to a Ni^I(cyclam) species, which undergoes CO_2 coordination followed by proton attack to the coordinated CO_2, and finally CO and OH^- are yielded after the second one-electron reduction. This reaction mechanism involves several points to be investigated, as follows: (1) the Ni^I–CO_2 complex has not been isolated, to our knowledge, whereas several electrochemical evidences have been reported,[6b,21] (2) very little has been known about the coordination geometry, electronic structure, and reactivity of the Ni^I–CO_2 complex, and (3) it is not clear whether protonation of the coordinated CO_2 ligand is necessary for this electrocatalytic reduction of CO_2 or not. Theoretical investigation is expected to offer useful information about these issues.

In our preliminary ab initio MO/SD-CI study,[22] several Ni^I– and Ni^{II}–CO_2 complexes, $Ni^IF(NH_3)_4(CO_2)$, $[Ni^I(NH_3)_4(CO_2)]^+$, and $[Ni^{II}F(NH_3)_4(CO_2)]^+$, were theoretically investigated as a model of an intermediate of electrocatalytic reduction of CO_2 by $NiCl_2$(cyclam), where $(NH_3)_4$ and F were employed as models of cyclam and Cl, respectively. We now report a more detailed ab initio MO/SD-CI study of the reaction mechanism of the CO_2 electrocatalytic reduction by $NiCl_2$(cyclam). The following issues are mainly discussed: (1) geometry, electronic structure, and reactivity of $Ni^IF(NH_3)_4(\eta^1\text{-}CO_2)$ and its protonated complex $[Ni^IF(NH_3)_4(\eta^1\text{-}CO_2H)]^+$, (2) energy change and electron redistribution caused by the second one-electron reduction, and (3) electronic states and coordinate bond of CO in $[Ni^{II}F(NH_3)_4(CO)]^+$. The emphasis of this work is to present several useful pieces of information for us to understand the reaction mechanism proposed by Sauvage et al.[6]

Computational Details

Spin-restricted ab initio MO and limited SD-CI calculations were carried out with the MELD program.[23] Two kinds of basis sets, BS-I and BS-II, were used. In the BS-I set with which SD-CI calculations were performed, the MIDI-4 basis sets[24] were used for C, O, and F, and the (4s/2s) set[25] was used for H of the CO_2H group, whereas the MINI-4 and (4s/1s)[26] sets were employed for N and H of NH_3, respectively. For Ni, Huzinaga's (13s 7p 5d) primitive set, proposed for the Ni $^3D(d^9s)$ state,[24] was augmented with a diffuse d primitive ($\zeta = 0.10$)[27] and three p primitives whose exponents were taken to be the same as the three most diffuse s primitives of Ni. The resultant (13s 10p 6d) primitives were contracted to [5s 4p 3d], i.e., minimal for all core orbitals, double-ζ for the 4s and 4p orbitals, and triple-ζ for the 3d orbital. In the BS-II set with which geometry optimization was performed, MINI-1 and (3s/1s) were used for N, F, and H of NH_3, respectively, to reduce computation time, whereas the same basis sets as in the BS-I were employed for the $Ni(CO_2)$ moiety.

Limited SD-CI calculations were carried out with a single Hartree–Fock (HF) configuration as a reference, where virtual orbitals were transformed to K orbitals[28] to improve the CI convergence and all core orbitals were excluded from the active space. All possible spin-adapted configurations were screened, on the basis of the second-order Rayleigh–Schrödinger perturbation theory,[29] to reduce numbers of configurations which undergo a variational SD-CI calculation. The threshold of energy used in the screening was 200 μhartrees. This value was not small but rather large; SD excitations remaining after the screening included about 85% of the estimated SD correlation energy. However, the smaller value of threshold led to too large numbers of configurations to perform the SD-CI calculation in some cases; even using this threshold, about 52 500 spin-adapted configurations remained after the screening in the $^3A_2$ state of $[Ni^{II}F(NH_3)_4(\eta^1\text{-}CO_2)]^+$. The influence of the energy threshold was examined in $[Ni^{II}F(NH_3)_4(\eta^1\text{-}CO_2)]^+$ taking the $^1A_1$ state; the binding energy of CO_2 coordination was −29.1 kcal/mol at 100 μhartrees, −28.6 kcal/mol at 150 μhartrees, and −28.9 kcal/mol at 200 μhartrees (a negative value of the binding energy means destabilization, and vice versa). Thus, the CO_2 binding energy hardly depends on the energy threshold, and therefore, relative stabilities of Ni^I– and Ni^{II}–CO_2 complexes examined seem to be reliably compared here.

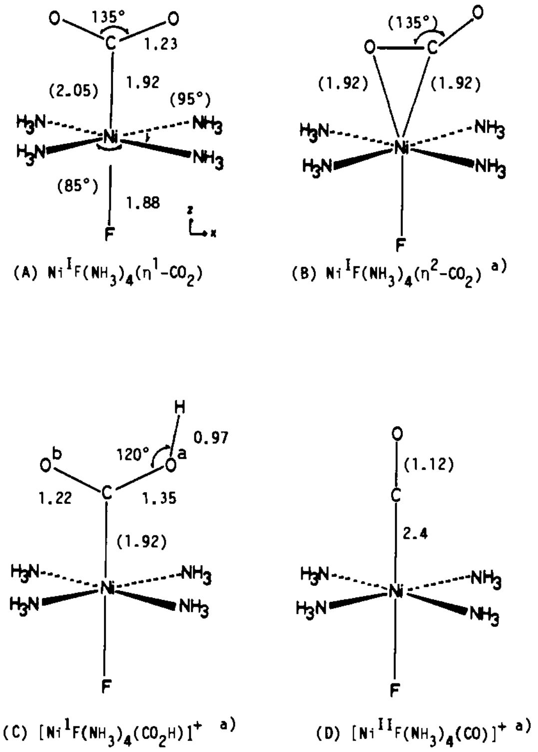

(A) $Ni^IF(NH_3)_4(\eta^1\text{-}CO_2)$ (B) $Ni^IF(NH_3)_4(\eta^2\text{-}CO_2)$ [a)]

(C) $[Ni^IF(NH_3)_4(CO_2H)]^+$ [a)] (D) $[Ni^{II}F(NH_3)_4(CO)]^+$ [a)]

Figure 1. Optimized structure of several Ni^I and Ni^{II} complexes examined. The superscript a indicates that the $Ni(NH_3)_4$ structure was assumed to be the same as that of $Ni^IF(NH_3)_4(\eta^1\text{-}CO_2)$. Assumed geometrical parameters which were taken from the experimental structure of a similar complex[20] are given in parentheses.

The remaining SD excited configurations underwent variational CI calculations. Thus, the obtained limited SD-CI correlation energy, E_t(lim SD-CI), was corrected by estimating the correlation energy arising from the discarded configuration functions, and then further correction was carried out by estimating the contribution of the higher order CI expansions,[30] to yield E_t(est full CI).

A CI wave function of $[Ni^IF(NH_3)_4(\eta^1\text{-}CO_2)]$ is briefly described here, as an example; C_0 is about 0.91, the second leading term is the $(20a_1)^2 \rightarrow (21a_1)^2$ excited configuration whose coefficient is about 0.11, and the other terms have coefficients smaller than 0.05. Occupation numbers of the $20a_1$ and $21a_1$ natural orbitals are 1.939 and 0.069, respectively. The $20a_1$ MO mainly involves the bonding interaction between Ni d_{z^2} and CO_2 π^* orbitals, and the $21a_1$ MO its antibonding counterpart. Thus, the Ni $d_{z^2} \rightarrow CO_2$ π^* back-bonding interaction is not described well at the HF level, but is improved by introduction of electron correlation. Similar improvement of the back-bonding interaction by electron correlation has been reported previously in several low-valent transition-metal complexes.[31,32]

The geometry of NH_3 was taken from an X-ray experimental work of a free NH_3.[33] The structure of the NiN_4 frame was taken from an

---

(18) (a) Ishida, H.; Tanaka, K.; Tanaka, T. *Chem. Lett.* **1987**, 1035. (b) Ishida, H.; Terada, T.; Tanaka, K.; Tanaka, T. *Inorg. Chem.* **1990**, *29*, 905.

(19) Silavwe, N. D.; Goldman, A. S.; Ritter, R.; Tyler, D. R. *Inorg. Chem.* **1989**, *28*, 1231.

(20) Lehn, J.-M.; Ziessel, R. *J. Organomet. Chem.* **1990**, *382*, 157.

(21) Schmidt, M. H.; Miskelly, G. M.; Lewis, N. S. *J. Am. Chem. Soc.* **1990**, *112*, 3420.

(22) Sakaki, S. *J. Am. Chem. Soc.* **1990**, *112*, 7813.

(23) Davidson, E. R.; McMurchie, L.; Elbert, S.; Langhoff, S. R.; Rawlings, D.; Feller, D. MELD; University of Washington, Seattle, WA; IMS Computer Center Library, No. 030.

(24) Huzinaga, S.; Andzelm, J.; Klobukowski, M.; Radzio-Andzelm, E.; Sakai, Y.; Tatewaki, H. *Gaussian Basis Sets for Molecular Calculations*; Elsevier: Amsterdam, 1984.

(25) Dunning, T. *J. Chem. Phys.* **1970**, *53*, 2823.

(26) Huzinaga, S. *J. Chem. Phys.* **1965**, *42*, 1293.

(27) This value was determined with the even-tempered criterion.

(28) Feller, D.; Davidson, E. R. *J. Chem. Phys.* **1981**, *84*, 3997.

(29) Langhoff, S. R.; Davidson, E. R. *Int. J. Quantum Chem.* **1974**, *8*, 61.

(30) Davidson, E. R.; Silver, D. W. *Chem. Phys. Lett.* **1977**, *52*, 403.

(31) Rohlfing, C. H.; Hay, P. J. *J. Chem. Phys.* **1985**, *83*, 4641.

(32) (a) Sakaki, S.; Ohkubo, K. *J. Phys. Chem.* **1989**, *23*, 5655. (b) Sakaki, S.; Koga, N.; Morokuma, K. *Inorg. Chem.* **1990**, *29*, 3110.

(33) Kuchitsu, K.; Guillory, J. P.; Bartell, L. S. *J. Chem. Phys.* **1968**, *49*, 2488.

Chart I

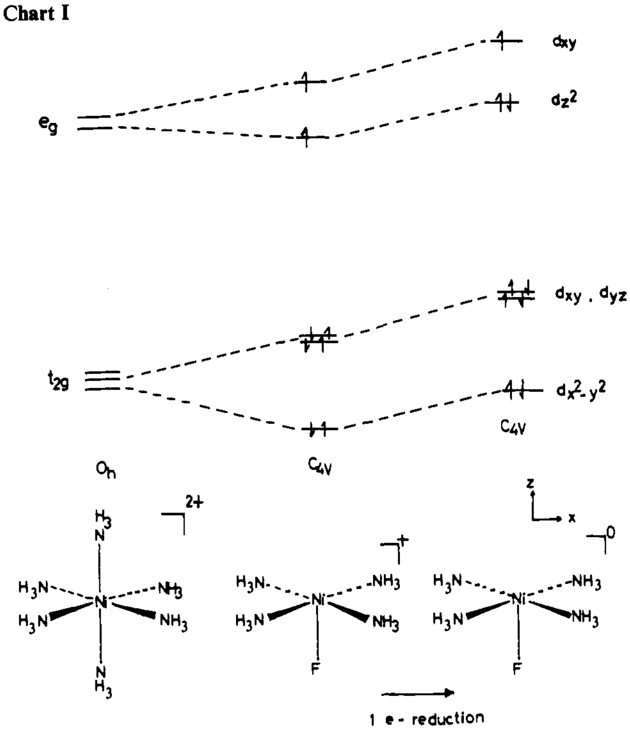

X-ray structure of [Ni(cyclam)]$(NO_3)_2$.[34] In $Ni^IF(NH_3)_4(\eta^1\text{-}CO_2)$, the Ni–C, C–O, and Ni–F distances and OCO angle were optimized independently at the HF level, by means of parabolic fitting of total energies. In $[Ni^I(NH_3)_5(\eta^1\text{-}CO_2)]^+$, the structure of $Ni(NH_3^{cis})_4(\eta^1\text{-}CO_2)$ was assumed to be the same as in $Ni^IF(NH_3)_4(CO_2)$ (NH_3^{cis} is cis-positioned to CO_2), while the Ni–N^{trans} was taken to be the same as the Ni–N^{cis} distance. The geometry of this complex was not optimized because the CO_2 binding energy of this complex was calculated to be much smaller than the usual coordinate bond (vide infra). The geometries of the η^2-side-on coordinated CO_2 complexes $[Ni^IF(NH_3)_4(\eta^2\text{-}CO_2)]$, $[Ni^I(NH_3)_4(\eta^2\text{-}CO_2)]^+$, and $[Ni^I(NH_3)_5(\eta^2\text{-}CO_2)]^+$ were not optimized because this coordination mode was calculated to be significantly unstable, in which the Ni–C distance and the CO_2 geometry were assumed to be the same as in $Ni^IF(NH_3)_4(\eta^1\text{-}CO_2)$. In the protonated CO_2 complex $[Ni^IF(NH_3)_4(CO_2H)]^+$, only the CO_2H part was optimized, where the Ni–C distance was assumed to be the same as in $[Ni^IF(NH_3)_4(\eta^1\text{-}CO_2)]$. The one-electron-reduced state of this complex was assumed to take the same structure as that of $[Ni^IF(NH_3)_4(CO_2H)]^+$. In $[Ni^{II}F(NH_3)_4(CO)]$, the structure of the $NiF(NH_3)_4$ moiety was assumed to be the same as that of $[Ni^IF(NH_3)_4(\eta^1\text{-}CO_2)]$, where the C–O distance was taken to be the same as the optimized one of a free CO molecule.[35] The Ni–CO distance was, however, optimized at the SD-CI level with the BS-I set because the CO coordination is repulsive at the HF level.

The optimized structures are displayed in Figure 1, together with the assumed structure of $[Ni^IF(NH_3)_4(\eta^2\text{-}CO_2)]$.

Results and Discussion

Prior to detailed discussion, possible electronic states of Ni^I and Ni^{II} complexes are briefly described here. When $Ni(NH_3)_6$ changes to $NiF(NH_3)_4$ by taking away an NH_3 ligand from the *z* axis and substituting another NH_3 ligand for F^-, d(e_g) orbitals are separated to d_{xy} and d_{z^2} and d(t_{2g}) orbitals to d_{xz}, d_{yz}, and $d_{x^2-y^2}$, as shown in Chart I (note the *x* and *y* axes bisect the NNiN angle). In the Ni^{II} complex which has 8 d electrons, three electronic states are possible; one is the triplet state in which both d_{z^2} and d_{xy} are singly occupied, the second is the singlet in which d_{z^2} is doubly occupied, and the last is the different singlet in which d_{xy} is doubly occupied. Although the first is the most stable in general, all three states are calculated in the Ni^{II} complex. When Ni^{II} is reduced to Ni^I, two kinds of doublet states are possible; in one, d_{xy} is singly occupied and d_{z^2} is doubly occupied, and in the other, d_{xy} is doubly occupied and d_{z^2} is singly occupied. The former is expected to be favorable for η^1-CO_2 coordination, but the latter to be favorable for the η^2-side-on CO_2 coordination. Thus, these two states are calculated.

Chart II

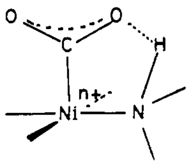

Table I. Relative Stabilities and CO_2 Binding Energies[a,b]

complex	state	relative energy (kcal/mol) HF	binding energy (kcal/mol) HF	binding energy (kcal/mol) SD-CI
$Ni^IF(NH_3)_4(\eta^1\text{-}CO_2)$	$^2A_2(d_{z^2}{}^2d_{xy}{}^1)$	0	22[c]	48[d]
	$^2A_1(d_{z^2}{}^1d_{xy}{}^2)$	27		
$[Ni^I(NH_3)_4(\eta^1\text{-}CO_2)]^+$	$^2A_2(d_{z^2}{}^2d_{xy}{}^1)$	0	−44[e]	−14[f]
	$^2A_1(d_{z^2}{}^1d_{xy}{}^2)$	62		
$[Ni^{II}F(NH_3)_4(\eta^1\text{-}CO_2)]^+$	$^1A_1(d_{z^2}{}^2d_{xy}{}^0)$	0	−80[g]	−29[h]
	$^1A_1(d_{z^2}{}^0d_{xy}{}^2)$	44		
	$^3A_2(d_{z^2}{}^1d_{xy}{}^1)$	−51	−96[i]	−21[j]
$[Ni^I(NH_3)_5(\eta^1\text{-}CO_2)]^+$	$^2A''(d_{z^2}{}^2d_{xy}{}^1)$		−18[h]	14[l]
$Ni^IF(NH_3)_4(\eta^2\text{-}CO_2)$	$^2A''(d_{z^2}{}^2d_{xy}{}^1)$	0	−130[m]	
	$^2A'(d_{z^2}{}^1d_{xy}{}^2)$	77	−29[n]	
$[Ni^I(NH_3)_4(\eta^2\text{-}CO_2)]^+$	$^2A''(d_{z^2}{}^2d_{xy}{}^1)$		−88[o]	
$[Ni^I(NH_3)_5(\eta^2\text{-}CO_2)]^+$	$^2A''(d_{z^2}{}^2d_{xy}{}^1)$		−74[p]	

[a] $E_t(R(Ni\text{–}CO_2) = 50\ Å) - E_t$(optimized structure). [b] *E*(est full CI) (see Computational Details in the text). [c] $E_t = -2016.4174$ hartrees. [d] $E_t = -2017.4063$ hartrees. [e] $E_t = -1916.8916$ hartrees. [f] $E_t = -1917.7618$ hartrees. [g] $E_t = -2016.1397$ hartrees. [h] $E_t = -2017.1327$ hartrees. [i] $E_t = -2016.2202$ hartrees. [j] $E_t = -2017.1658$ hartrees. [k] $E_t = -1972.9709$ hartrees. [l] $E_t = -1973.9149$ hartrees. [m] $E_t = -2016.1758$ hartrees. [n] $E_t = -2016.2987$ hartrees. [o] $E_t = -1992.8220$ hartrees. [p] $E_t = -1972.8818$ hartrees.

Coordination Structure and CO_2 Binding Energy of $Ni^IF(NH_3)_4(CO_2)$, $[Ni^I(NH_3)_4(CO_2)]^+$, $[Ni^{II}F(NH_3)_4(CO_2)]^+$, and $[Ni^I(NH_3)_5(CO_2)]^+$.

Sauvage et al. proposed the bifunctional η^1-CO_2 complex of $[Ni^I(cyclam)]^+$ as an intermediate,[6b] which is stabilized by an additional interaction between $O^{\delta-}$ of CO_2 and $H^{\delta+}$–N of cyclam, as well as the Ni–C interaction (see Chart II).

The coordination structure of $Ni^IF(NH_3)_4(\eta^1\text{-}CO_2)$ was optimized, as shown in Figure 1A. Of two possible electronic states, $^2A_2(d_{z^2}{}^2d_{xy}{}^1)$ is significantly more stable than $^2A_1(d_{z^2}{}^1d_{xy}{}^2)$ (see Table I), probably because the η^1-CO_2 coordination needs the doubly occupied d_{z^2} orbital (vide infra) and the d_{xy} orbital is considerably destabilized by an antibonding interaction with lone pairs of NH_3. Thus, the optimization is carried out for the $^2A_2$ state. The optimized structure (Figure 1A) resembles very much the well-known η^1-CO_2 complexes $RhCl(diars)_2(CO_2)$[36] and M[Co(R-salen)(CO_2)][37] on the points of the C–O distance, the OCO angle, and the staggered orientation of CO_2 to the Ni–N bond. The binding energy is calculated to be 22 kcal/mol at the HF level and 48 kcal/mol at the SD-CI level after Davidson's correction, as listed in Table I. These values suggest that the η^1-CO_2 coordination to Ni^I is as strong as the usual coordinate bond.

The $H^{\delta+}$–$O^{\delta-}$ interaction between N–$H^{\delta+}$ of cyclam and $O^{\delta-}$ of CO_2 has been proposed to stabilize the CO_2 coordination, as described above.[6b] We investigate here how much this $H^{\delta+}$–$O^{\delta-}$ interaction contributes to the η^1-CO_2 coordination. Several coordination structures with and without $H^{\delta+}$–$O^{\delta-}$ interaction (**1**–**3**

---

[34] (a) Thom, V. J.; Fox, C. C.; Boeyens, J. C. A.; Hancock, R. D. *J. Am. Chem. Soc.* **1984**, *106*, 5947. (b) See **3a** for the orientation of NH_3. By adopting this orientation, **3** takes the C_{2v} symmetry, which reduces computation time.

[35] The Ni–F and C–O distances of $[Ni^{II}F(NH_3)_4(CO)]^+$ were optimized with a MINI-1 set for F. The optimized Ni–F (1.87 Å) and C–O (1.12 Å) value, however, deviate little from the Ni–F distance (1.88 Å) of $Ni^IF(NH_3)_4(\eta^1\text{-}CO_2)$ and the C–O distance (1.12 Å) of the free CO molecule.

[36] Calabrese, J. C.; Herskovitz, T.; Kinney, J. B. *J. Am. Chem. Soc.* **1983**, *105*, 5914.

[37] (a) Facinetti, G.; Floriani, C.; Zanazzi, P. F. *J. Am. Chem. Soc.* **1978**, *100*, 7405. (b) Fachinetti, G.; Floriani, C.; Zanazzi, P. F.; Zanarim, A. R. *Inorg. Chem.* **1979**, *18*, 3469.

Chart III

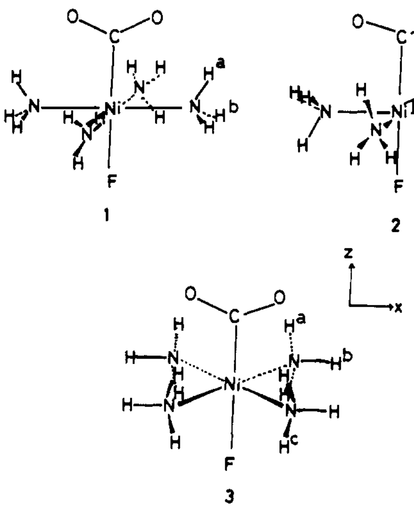

3a: CO_2 on the yz-plane
3b: CO_2 on the xz-plane

Table II. Mulliken Populations of $Ni^IF(NH_3)_4(\eta^1\text{-}CO_2)$ with and without $H^{\delta+}\text{–}O^{\delta-}$ Interaction[a]

	eclipsed[a]		staggered[a]	
	1	**2**	**3a**	**3b**
$R(H^a\text{–}O)$[b] (Å)	1.95 (2)	2.32 (2)	2.30 (4)	2.60 (4)
BE[c] (kcal/mol)	9.8	9.8	22.0	19.2
populations				
Ni	26.150	26.119	26.206	26.203
NH_3 on x	10.078	10.103	10.071	10.075
H^a[d]	0.716	0.760	0.728	0.747
H^b	0.765	0.759	0.766	0.755
H^c			0.745	0.748
NH_3 on y	10.107	10.095	10.071	10.075
CO_2	22.849	22.858	22.877	22.862
C	5.541	5.832	5.710	5.729
O	8.541	8.513	8.584	8.566

[a] See Chart III for **1**, **2**, **3a**, and **3b**. [b] The numbers of H^a which can form the $H^{\delta+}\text{–}O^{\delta-}$ interaction are given in parentheses. [c] $E_t[NiF(NH_3)_4] + E_t(CO_2)_{eq} - E_t[NiF(NH_3)_4(\eta^1\text{-}CO_2)]$. [d] See Chart II for H^a, H^b, and H^c (H^c is defined only in **3**).

in Chart III) are calculated at the HF level.[38] In **1**, CO_2 is eclipsed to the Ni–N bond in which H of NH_3 is placed close to O of CO_2 to mimic the $H^{\delta+}\text{–}O^{\delta-}$ interaction of Chart II. In **2**, CO_2 is eclipsed to the Ni–N bond like in **1**, but NH_3 is rotated so as to keep H at a distance from O. In **3**, CO_2 is staggered to Ni–N bonds.[38b] If the $H^{\delta+}\text{–}O^{\delta-}$ interaction exists, the CO_2 and NH_3 groups are polarized by this interaction, which increases the positive charge of H^a and negative charge of O (see Chart III for H^a). Mulliken populations, given in Table II, show interesting contrast between **1** and **2**; in **1**, the H^a atomic population is considerably smaller than that of H^b, whereas all H atoms have similar atomic population in **2**. Furthermore, the O atomic population is larger in **1** than in **2**. These results suggest that the $H^{\delta+}\text{–}O^{\delta-}$ interaction is formed in **1** but not in **2**. Nevertheless, **1** and **2** have almost the same binding energy of CO_2. In the staggered structure, two kinds of conformation were examined; **3a** in which CO_2 is on the yz plane has a shorter H^a–O distance than **3b** in which CO_2 is on the xz plane (see Table II for the H^a–O distance and Chart III for details of the structure). In **3b** whose binding energy is slightly smaller than that of **3a**, all three H atoms have similar electron population, suggesting the absence of $H^{\delta+}\text{–}O^{\delta-}$ interaction. Nevertheless, **3b** is more stable than **1**, whereas **1** involves the $H^{\delta+}\text{–}O^{\delta-}$ interaction. In **3a** which exhibits the greatest binding energy, the H^a atom is more positively charged than the others and the O atom is very negatively charged, suggesting the presence of $H^{\delta+}\text{–}O^{\delta-}$ interaction. Thus, the $H^{\delta+}\text{–}O^{\delta-}$ interaction is considered to contribute to the greater stabilization of **3a** than that of **3b**. However, the above-mentioned comparisons between **1** and **2** and between **1** and **3b** suggest that the $H^{\delta+}\text{–}O^{\delta-}$ interaction is not definitively important in CO_2 coordination.

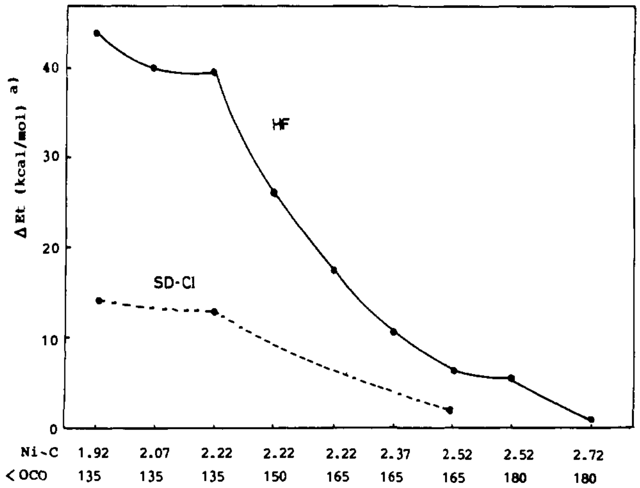

Figure 2. Energy change caused by CO_2 dissociation from Ni in $[Ni(NH_3)_4(\eta^1\text{-}CO_2)]^+$. The standard (energy 0) is taken for the infinite separation between Ni and CO_2 (50 Å).

In $[Ni^I(NH_3)_4(\eta^1\text{-}CO_2)]^+$, the $^2A_2$ state is more stable than the $^2A_1$ state by ca. 62 kcal/mol, as shown in Table I. The binding energy at $^2A_2$ is, however, calculated to be significantly negative at both the HF level (−44 kcal/mol) and the SD-CI level (−22 kcal/mol), where the structure of the Ni–CO_2 frame is taken to be the same as in $Ni^IF(NH_3)_4(\eta^1\text{-}CO_2)$. In order to ascertain that CO_2 cannot coordinate to Ni^I in this complex, the CO_2 dissociation process was examined in detail; the Ni–C distance is lengthened first from 1.91 to 2.22 Å with the CO_2 geometry fixed, the OCO angle was opened at R(Ni–C) = 2.22 Å, the Ni–C distance was lengthened again to 2.52 Å with the CO_2 geometry fixed, the OCO angle is opened to 180° at R(Ni–C) = 2.52 Å, and finally the Ni–C distance was lengthened to 2.72 Å with the CO_2 geometry fixed to the structure of its free molecule, as shown in Figure 2. All these geometry changes lead to stabilization in energy at both the HF and SD-CI levels, and furthermore, the most separated structure (R(Ni–C) = 2.72 Å) is still less stable than the sum of $[Ni^I(NH_3)_4]^+$ and CO_2. Thus, it can be concluded that CO_2 does not coordinate to $[Ni(NH_3)_4]^+$.

In $[Ni^I(NH_3)_5(\eta^1\text{-}CO_2)]^+$, the $^2A''(d_{z^2}{}^2d_{xy}{}^1)$ state was calculated because this state corresponds to the stable $^2A_2$ state of $Ni^IF(NH_3)_4(\eta^1\text{-}CO_2)$. The calculated binding energy is negative at the HF level but positive at the SD-CI level (Table I). This positive binding energy is, however, much smaller than that of $Ni^IF(NH_3)_4(\eta^1\text{-}CO_2)$. These results suggest an anionic ligand is much more favorable for the $Ni^I(\eta^1\text{-}CO_2)$ complex than a neutral ligand (the reason will be discussed later).

CO_2 coordination to Ni^{II} is then examined in $[Ni^{II}F(NH_3)_4(\eta^1\text{-}CO_2)]^+$. Of three possible electronic states, $^3A_2(d_{z^2}{}^1d_{xy}{}^1)$ is the most stable, and $^1A_1(d_{z^2}{}^2d_{xy}{}^0)$ is the next stable at both HF and SD-CI levels. The CO_2 binding energies are calculated to be significantly negative at both $^3A_2$ and $^1A_1$ states, as listed in Table I.

The possibility of the η^2-side-on CO_2 coordination to Ni^I is finally investigated. In $Ni^IF(NH_3)_4(\eta^2\text{-}CO_2)$, the $^2A''(d_{z^2}{}^2d_{xy}{}^1)$ state is calculated to be more stable than the $^2A'(d_{z^2}{}^1d_{xy}{}^2)$ state (Table I). The CO_2 binding energy is significantly negative at the HF level in both electronic states. Also, $[Ni^I(NH_3)_4(\eta^2\text{-}CO_2)]^+$ and $[Ni^I(NH_3)_5(\eta^2\text{-}CO_2)]^+$ exhibit significantly negative binding energy, where the $^2A''(d_{z^2}{}^2d_{xy}{}^1)$ state is calculated like in $Ni^IF(NH_3)_4(\eta^2\text{-}CO_2)$. These results mean that the η^2-side-on coor-

---

[38] (a) The structure of the $NiF(CO_2)$ frame was assumed to be the same as in the optimized structure of $Ni^IF(NH_3)_4(\eta^1\text{-}CO_2)$, while the NNiN angle was taken to be 90° to reduce computation time by adopting the C_{2v} symmetry. Calculations were carried out on the $^2A_2(d_{z^2}{}^2d_{xy}{}^1)$ state. (b) The orientation of NH_3 in **3** differs from **1** and **2**; in **3**, the H^b atom is placed on the xy plane to adopt the C_{2v} symmetry (see ref 34b for the reason for taking this symmetry).

Table III. Mulliken Population Changes[a] Caused by η^1-CO_2 Coordination

	$Ni^IF(NH_3)_4(\eta^1\text{-}CO_2)$ $^2A_2(d_{z^2}{}^2d_{xy}{}^1)$	$[Ni^I(NH_3)_4(\eta^1\text{-}CO_2)]^+$ $^2A_2(d_{z^2}{}^2d_{xy}{}^1)$	$[Ni^{II}F(NH_3)_4(\eta^1\text{-}CO_2)]^+$ $^3A_2(d_{z^2}{}^1d_{xy}{}^1)$	$[Ni^I(NH_3)_5(\eta^1\text{-}CO_2)]^+$ $^2A''(d_{z^2}{}^2d_{xy}{}^1)$
Ni	−0.687	−0.351	−0.098	−0.541
	(26.896)[b]	(26.778)	(26.294)	(26.585)
s	0.030	−0.002	+0.060	+0.039
p	−0.166	−0.052	−0.144	−0.059
d	−0.551	−0.297	−0.014	−0.522
F	−0.066		−0.052	−0.011 (NH_3^{trans})
NH_3	−0.031	−0.016	−0.008	−0.025
CO_2	0.872	0.409	0.109	0.657
C	0.380	0.178	0.210	0.311
O	0.246	0.116	−0.050	0.173

[a] SD-CI calculation. Positive value means an increase in population. [b] The Ni atomic population before CO_2 coordination.

dination of CO_2 is not stable. The SD-CI calculation was not carried out because the binding energy was too negative.

Of these Ni^I– and Ni^{II}–CO_2 complexes examined, $Ni^IF(NH_3)_4(\eta^1\text{-}CO_2)$ and $[Ni^I(NH_3)_5(\eta^1\text{-}CO_2)]^+$ are calculated to be stable,[39] whereas the latter is much less stable than the former. This means that coordination of an anion ligand is favorable for stabilizing the $Ni^I(\eta^1\text{-}CO_2)$ complex. Probably, adsorption of the Ni^I complex to an anode surface would cause similar effects on the Ni^I–CO_2 complex like coordination of an anion ligand and would yield a stable $Ni^I(\eta^1\text{-}CO_2)$ complex (vide infra).

Factors Stabilizing CO_2 Coordination. The stability of the transition-metal CO_2 complex is, in general, discussed in terms of the nature of the frontier orbital of the metal moiety.[40] The HOMO of $Ni^IF(NH_3)_4$, $[Ni^I(NH_3)_4]^+$, and $[Ni^I(NH_3)_5]^+$ is a singly occupied d_{xy} orbital. However, this orbital plays an important role not in CO_2 coordination but in NH_3 coordination. The d_{z^2}, d_{xz}, and d_{yz} orbitals are expected to be important because they extend toward CO_2. The d_{z^2} orbital is the next HOMO, but the d_{xz} and d_{yz} orbitals lie lower in energy than the d_{z^2} orbital by ca. 2.5 eV, as shown in Chart I. This situation favors the η^1-C coordination but disfavors the η^2-side-on coordination, because the η^1-C coordination needs a strong charge-transfer interaction from the Ni d_{z^2} to the CO_2 π^* orbital but the η^2-side-on coordination requires a different kind of charge transfer from Ni d_π to CO_2 π^*.[40] This is the reason that $Ni^IF(NH_3)_4(\eta^2\text{-}CO_2)$, $[Ni^I(NH_3)_4(\eta^2\text{-}CO_2)]^+$, and $[Ni^I(NH_3)_5(\eta^2\text{-}CO_2)]^+$ are unstable.

Then, let us discuss factors stabilizing the η^1-CO_2 coordination. The η^1-CO_2 coordination needs a doubly occupied $d\sigma$ orbital lying high in energy, because the charge transfer from the Ni d_σ to the CO_2 π^* orbital is indispensable for stabilizing this coordination mode. In the stable $Ni^IF(NH_3)_4(\eta^1\text{-}CO_2)$, the CO_2 electron population substantially increases and the Ni d orbital population considerably decreases upon CO_2 coordination to Ni (Table III). This strong charge-transfer interaction is easily interpreted in terms of the Ni d_{z^2} orbital lying high in energy (−5.0 eV) in $Ni^IF(NH_3)_4$. In the unstable $[Ni^I(NH_3)_4(\eta^1\text{-}CO_2)]^+$ and $[Ni^{II}F(NH_3)_4(\eta^1\text{-}CO_2)]^+$, on the other hand, the CO_2 electron population increases to a lesser extent than in the stable $Ni^IF(NH_3)_4(\eta^1\text{-}CO_2)$, because the Ni d_{z^2} orbital lies low in energy in $[Ni^I(NH_3)_4]^+$ (−12.9 eV) and $[Ni^{II}F(NH_3)_4]^+$ (−14.6 eV). These results suggest that $Ni^IF(NH_3)_4(\eta^1\text{-}CO_2)$ is stabilized by a strong charge-transfer interaction from Ni d_{z^2} to CO_2 π^*, whereas $[Ni^I(NH_3)_4(\eta^1\text{-}CO_2)]^+$ and $[Ni^{II}F(NH_3)_4(\eta^1\text{-}CO_2)]^+$ are stabilized to a lesser extent by this interaction. In the less stable $[Ni(NH_3)_5(\eta^1\text{-}CO_2)]^+$, however, the CO_2 electron population significantly increases upon CO_2 coordination to Ni^I, to a much greater extent than in $[Ni^I(NH_3)_4(\eta^1\text{-}CO_2)]^+$ and $[Ni^{II}F(NH_3)_4(\eta^1\text{-}CO_2)]^+$, but to a lesser extent than in $Ni^IF(NH_3)_4(\eta^1\text{-}CO_2)$. This result is easily interpreted in terms of the Ni d_{z^2} orbital energy; the Ni d_{z^2} orbital in $[Ni(NH_3)_5]^+$ lies higher in energy (−10.7 eV) than in $[Ni^{II}F(NH_3)_4]^+$ and $[Ni^I(NH_3)_4]^+$ but lower than in $Ni^IF(NH_3)_4$. A contrast between stable $Ni^IF(NH_3)_4(\eta^1\text{-}CO_2)$ and others is that the former has a neutral metal fragment but the latters have a positively charged one. The positively charged metal fragment would cause electrostatic repulsion with the dipole moment of the bending CO_2 ligand. Thus, the less stability of $[Ni^I(NH_3)_5(\eta^1\text{-}CO_2)]^+$ than that of $Ni^IF(NH_3)_4(\eta^1\text{-}CO_2)$ would result from the weaker charge-transfer interaction and the stronger electrostatic repulsion between the metal fragment and η^1-CO_2.

In conclusion, coordination of an anion ligand neutralizes the positive charge of Ni^I to reduce the charge–dipole repulsion, and at the same time, pushes up the d_{z^2} orbital in energy to enhance the charge transfer from Ni d_{z^2} to CO_2. On the other hand, coordination of a neutral ligand pushes up the d_{z^2} orbital in energy to a lesser extent than an anion ligand and cannot neutralize the positive charge of Ni^I. Thus, coordination of an anion ligand is favorable for the formation of the stable $Ni^I(\eta^1\text{-}CO_2)$ complex. Adsorption of $[Ni^I(cyclam)]^+$ onto the anode surface would be expected to stabilize $[Ni^I(cyclam)(\eta^1\text{-}CO_2)]^+$ like the anion coordination, because such an anode surface would be negatively charged.

Electron Distribution and Reactivity of CO_2 in $Ni^IF(NH_3)_4(\eta^1\text{-}CO_2)$. Because $NiCl_2$(cyclam) is used in experiment, an anionic Cl ligand is considered to be able to coordinate to $Ni^I(cyclam)(\eta^1\text{-}CO_2)$. Hereafter, we investigate $Ni^IF(NH_3)_4(\eta^1\text{-}CO_2)$ as a model of an intermediate.

As briefly discussed above, this complex is stabilized by substantial charge transfer from Ni d_σ to CO_2 π^*. On the basis of Mulliken populations (Table III), such charge transfer accumulates electrons on the C and O atoms, while electron population decreases on the Ni d orbital, F, and NH_3. This means that not only the Ni d orbital but also NH_3 and F^- ligands supply electrons for CO_2. Difference density maps, shown in Figure 3A,B, offer a more clear picture of this charge transfer. Electron density accumulates around the C and O atoms but decreases around Ni, F, and NH_3, which agrees with a feature from the Mulliken population. Interestingly, electron density increases around the O atom to a similar extent to that around the C atom.[41] This feature cannot be interpreted in terms of simple charge transfer from Ni d_{z^2} to CO_2 π^*, because the simple charge transfer in-

---

(39) Some of the η^1-CO_2 complexes do not satisfy the 18 electron rule; for instance, $RhCl(diars)_2(\eta^1\text{-}CO_2)$[36] has 20 electrons around Rh, if we consider η^1-CO_2 as a two-electrons donor. However, η^1-CO_2 is strongly electron-accepting, and accepted electrons are distributed not only on the C atom but also on the O atoms. If η^1-CO_2 is considered as an electron acceptor, $RhCl(diars)_2(\eta^1\text{-}CO_2)$ has 18 electrons around Rh. $Ni^IF(NH_3)_4(\eta^1\text{-}CO_2)$ has 19 electrons around Ni, even if η^1-CO_2 is considered as an electron acceptor. This complex has an odd electron on the d_{xy} orbital (see Figure 1 for coordinate system). Because of this odd electron, this complex does not satisfy the 18 electron rule. However, coordination of cyclam would not be disturbed very much by this electron, because cyclam has strong coordinating ability to various metals. Thus, dissociation of NH_3 was not examined in our calculation, but NH_3 was fixed at the experimental position.[34] Probably, this is one of the reasons that $Ni^IF(NH_3)_4(\eta^1\text{-}CO_2)$ is calculated to be stable.

(40) (a) Sakaki, S.; Kitaura, K.; Morokuma, K. *Inorg. Chem.* **1982**, *21*, 760. (b) Sakaki, S.; Dedieu, A. *Inorg. Chem.* **1987**, *26*, 3278. (c) Sakaki, S. In *Stereochemical Control, Bonding and Steric Rearrangements*; Bernal, I., Ed.; Elsevier: Amsterdam, 1990; Vol. 4, pp 95–177.

(41) (a) The C atomic population increases more than the O atomic population, which slightly differs from the result of the difference density map. However, the results from the difference density map seem more reliable than those from the Mulliken population because the Mulliken population becomes unreasonable due to the counterintuitive orbital mixing[41b] when the system involves diffuse orbitals like transition metals. (b) Ammeter, J. H.; Burgi, H.-B.; Thibeault, J. C.; Hoffmann, R. *J. Am. Chem. Soc.* **1978**, *100*, 3686. Whangbo, M.-H.; Hoffmann, R. *J. Chem. Phys.* **1978**, *68*, 5398.

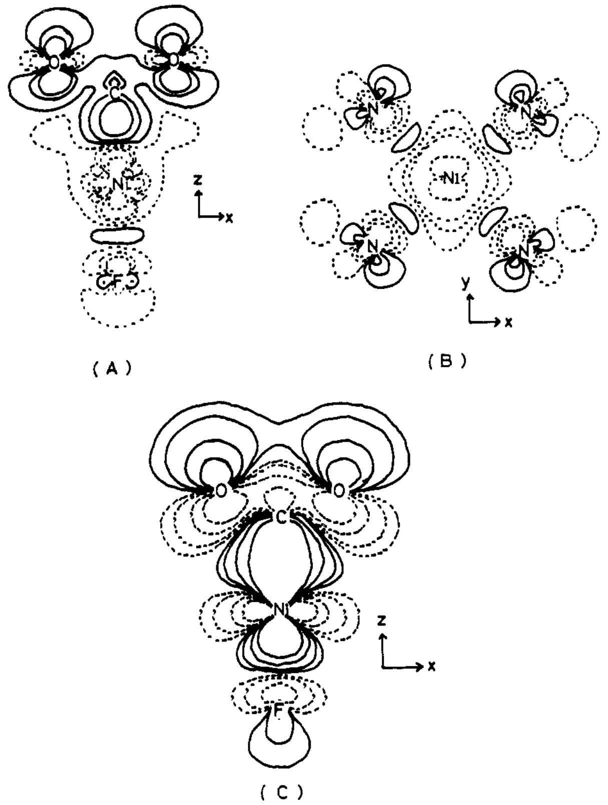

(A) (B)

(C)

Figure 3. Difference density maps A (yz plane) and B (xy plane) (±0.05, ±0.01, ±0.005) and Contour map C (xz plane) (±0.10, ±0.05, ±0.02, ±0.01) of the $20a_1$ natural orbital arising from the HOMO of [$Ni^IF(NH_3)_4(\eta^1\text{-}CO_2)$]: solid lines, positive value; dashed lines, negative value.

creases electron density on the C atom more than the O atom (note the C p_π orbital contributes more to the π^* orbital than the O p_π orbital does (see the π^* orbital shown in Chart IV)). Thus, the considerably large accumulation of the density around the O atom suggests that not a simple charge transfer from Ni d_{z^2} to CO_2 π^* but the other kind of interaction is involved in the CO_2 coordinate bond.

Electron distribution is considered, in general, to be much influenced by the nature of the HOMO. We examine here not the HOMO but the natural orbital (NMO) arising from the HOMO because electron distribution is discussed at the CI level. The $20a_1$ NMO mainly arises from the HOMO; the contribution of the HOMO is about 80%. As is shown by a contour map (Figure 3C), this orbital consists of the Ni d_{z^2} orbital and the deformed π^* orbital of CO_2 in which the C p_π orbital is diminished in size but the O p_π orbital is enhanced. This means that occupation of the $20a_1$ NMO increases the electron density on the O atom more than the C atom. Because its occupation number is 1.939, the feature of the $20a_1$ NMO is considered a major cause for the remarkable accumulation of the density around the O atom. Because the $20a_1$ NMO mainly consists of the HOMO (vide supra), the orbital mixing in the HOMO is considered to result in this characteristic feature of the $20a_1$ NMO; the Ni d_{z^2} and CO_2 π and π^* can mix to each others because they are in the a_1 representation of the C_{2v} symmetry (note the $Ni(\eta^1\text{-}CO_2)$ moiety has the C_{2v} symmetry). As previously discussed,[42] the Ni d_{z^2} orbital interacts with the less stable π^* orbital of CO_2 in a bonding way but with the more stable π orbital of CO_2 in an antibonding way, as shown in Chart IV. Consequently, the O p_π orbital is enhanced but the C p_π orbital is diminished in the HOMO, which yields the interesting feature of the $20a_1$ NMO shown by the contour map (Figure 3C).

The above-mentioned electron distribution and the feature of the HOMO offer a useful information about reactivity of the

Chart IV

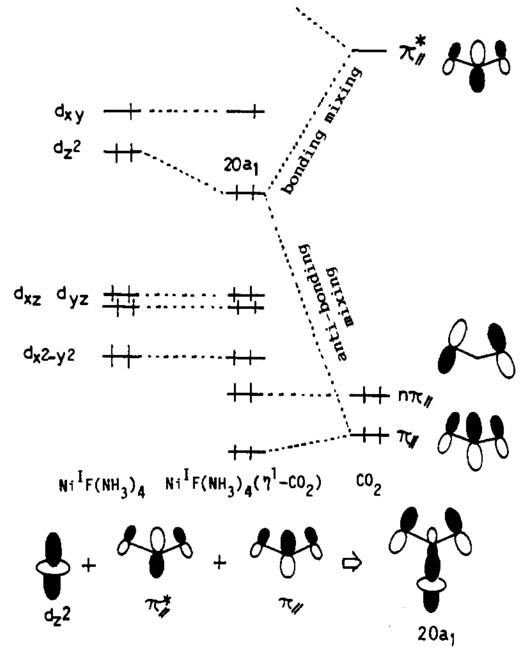

coordinated CO_2 ligand. The HOMO of the free CO_2 molecule is a nonbonding π orbital and lies at −14.6 eV. On the other hand, the HOMO of $Ni^IF(NH_3)_4(\eta^1\text{-}CO_2)$ consists of a considerably large p_π orbital of O and lies at −8.2 eV. Furthermore, electron density accumulates on the O atom, due to the above-mentioned orbital mixing. Thus, the coordinated CO_2 ligand is considered to be activated for an electrophile from viewpoints of frontier and charge controls.

Protonated [$Ni^IF(NH_3)_4(CO_2H)$]$^+$ Complex. In this complex, $^2A''(d_{z^2}{}^2d_{xy}{}^1)$ is calculated to be more stable than $^2A'(d_{z^2}{}^1d_{xy}{}^2)$ by 44 kcal/mol at the HF level, probably because a strongly antibonding orbital between d_{xy} and NH_3 is doubly occupied in the latter. The optimized structure of the $Ni\text{-}CO_2H$ frame (Figure 1C) exhibits features of a typical carboxyl group: (1) the $C\text{—}O^a$ and $C\text{—}O^b$ distances correspond to the C—O single bond and C═O double bond, respectively (see Figure 1C for O^a and O^b), (2) the CO^aH angle is 120°, exhibiting the typical sp^2 character of O^a, and (3) the $O^a\text{–}H$ distance agrees well with an experimental value. The optimized structure of the CO_2H group resembles the experimental structure of $Pt\text{-}CO_2H$ in the Pt^{II} complex.[43]

Mulliken population changes caused by proton attack are given in Table V. The H^+ receives a population of 0.533 upon attacking CO_2, while the electron population of CO_2 does not decrease but slightly increases unexpectedly. On the other hand, the Ni atomic population, in particular the Ni d orbital population, significantly decreases, and populations of F and NH_3 slightly decrease. Thus, charge transfer from CO_2 to proton is enhanced by the electron supply from Ni to CO_2. This electron flow is again helped by the electron supply from F and NH_3 to Ni.

The energy stabilization by protonation is 212 kcal/mol at the HF level and 249 kcal/mol at the SD-CI level. Although these values are overestimated because attack of a naked proton is calculated, these values might be compared with the energy stabilization by protonation of CO_2 in $RhCl(AsH_3)_4(\eta^1\text{-}CO_2)$.[42] In the latter, energy stabilization by protonation was calculated to be about 186 kcal/mol at the HF level and 191 kcal/mol at the MP2 level (note only a rough comparison is possible because basis sets and calculation methods are different between this work and ref 42). The stabilization energy in $Ni^IF(NH_3)_4(\eta^1\text{-}CO_2)$ is not smaller than that in $RhCl(AsH_3)_4(\eta^1\text{-}CO_2)$ which has been reported to easily undergo electrophilic attack.[36] This suggests that the protonation of $Ni^IF(NH_3)_4(\eta^1\text{-}CO_2)$ is a facile reaction.

---

(42) Sakaki, S.; Aizawa, T.; Koga, N.; Morokuma, K.; Ohkubo, K. *Inorg. Chem.* **1989**, *28*, 103.

(43) Bennett, M. A.; Robertson, G. B.; Rokicki, A.; Wickramasinghe, W. A. *J. Am. Chem. Soc.* **1988**, *110*, 7098.

Table IV. Relative Stabilities of Several Electronic States of $[NiF(NH_3)_4(CO_2)]^-$, $[NiF(NH_3)_4(CO_2H)]^+$, and $NiF(NH_3)_4(CO_2H)$ (kcal/mol)

		HF	SD-CI[a]
$[NiF(NH_3)_4(\eta^1\text{-}CO_2)]^-$	$^1A_1(d_{z^2}{}^2d_{xy}{}^2)$	0.0[b]	
	$^3A_2(d_{z^2}{}^2d_{xy}{}^1 21a_1{}^1)$	123.5	
	$^3B_2(d_{z^2}{}^2d_{xy}{}^1 11b_1{}^1)$	114.8	
	$^3B_1(d_{z^2}{}^2d_{xy}{}^1 14b_2{}^1)$	120.8	
$[NiF(NH_3)_4(CO_2H)]^+$	$^2A''(d_{z^2}{}^2d_{xy}{}^1)$	0.0[c]	
	$^2A'(d_{z^2}{}^1d_{xy}{}^2)$	44.0	
$NiF(NH_3)_4(CO_2H)$	$^3A'(d_{z^2}{}^2d_{xy}{}^1 21a_1{}^1)$	0.0[d]	0.0[e]
	$^1A''(d_{z^2}{}^2d_{xy}{}^2)$	60.1	38.4
$[NiF(NH_3)_4(CO)]^{+}$[f]	$^3A_2(d_{z^2}{}^1d_{xy}{}^1)$	0.0[g]	0.0[h]
	$^1A_1(d_{z^2}{}^2d_{xy}{}^0)$	81.7	58.2

[a] *E*(est full CI). See Computational Details in the text. [b] E_t = −2016.8086 hartrees. [c] E_t = −2016.3429 hartrees. [d] E_t = −2017.0677 hartrees. [e] E_t = −2017.9495 hartrees. [f] *R*(Ni–CO) = 2.1 Å. [g] E_t = −1941.6012 hartrees. [h] E_t = −1942.3716 hartrees.

Table V. Changes in Mulliken Populations Caused by Protonation of $Ni^IF(NH_3)_4(\eta^1\text{-}CO_2)$ and the Second One-Electron Reduction of $[Ni^IF(NH_3)_4(CO_2H)]^+$

	$Ni^IF(NH_3)_4$-$(\eta^1\text{-}CO_2)$	$[NiF(NH_3)_4$-$(CO_2H)]^+$	$NiF(NH_3)_4$-(CO_2H)
Ni	26.209	25.935 (−0.274)[a]	26.058 (+0.123)[b]
d	7.982	7.650 (−0.332)	7.876 (+0.226)
F	9.622	9.557 (−0.065)	9.648 (+0.091)
NH_3[c]	10.072	10.022 (−0.050)	10.106 (+0.083)
CO_2	22.872	22.886 (+0.014)	23.233 (+0.347)
C	5.711	5.761 (+0.050)	5.956 (+0.195)
O^a[d]	8.580	8.686 (+0.100)	8.704 (+0.018)
O^b[d]	8.580	8.439 (−0.141)	8.573 (+0.134)
H		0.533 (+0.533)	0.634 (+0.101)

[a] Change caused by the protonation. [b] Change caused by the one-electron reduction. [c] Averaged value of two different NH_3. [d] See Figure 1C for O^a etc.

Second One-Electron Reduction of Ni^I Complexes. Reduction of CO_2 to CO needs two electrons. The first electron is used for reduction of Ni^{II} to Ni^I. In the mechanism proposed by Sauvage et al., the second reduction occurs after the protonation of CO_2. Here, we investigate the second reduction.

Relative stabilities of several electronic states are examined first in $[NiF(NH_3)_4(\eta^1\text{-}CO_2)]^-$ and $NiF(NH_3)_4(CO_2H)$ which are considered as possible products of the second one-electron reduction. In $[NiF(NH_3)_4(\eta^1\text{-}CO_2)]^-$, the $^1A_1$ state is calculated to be the most stable of four electronic states, as shown in Table IV. In $NiF(NH_3)_4(CO_2H)$, on the other hand, the triplet state is more stable than the singlet at both HF and SD-CI levels. The energy change caused by the second reduction is calculated on these stable electronic states. As shown in Figure 4, one-electron reduction of $[Ni^IF(NH_3)_4(\eta^1\text{-}CO_2)]$ results in energy destabilization of 47 kcal/mol at the HF level and 81 kcal/mol at the SD-CI level. The reduction of $[NiF(NH_3)_4(CO_2H)]^+$, on the other hand, causes energy stabilization of 163 kcal/mol at the HF level and 92 kcal/mol at the SD-CI level. This means that the protonation of CO_2 is indispensable to the second reduction. In protic solvents, the second reduction is easily carried out because protonation is expected to occur very easily. In aprotic solvents, however, the second one-electron reduction is considered to be difficult because the Ni^I–CO_2 complex cannot undergo protonation.

Compared to the first one-electron reduction, the second reduction causes smaller stabilization in energy, as shown in Figure 4. This suggests that the second reduction needs more negative potential than the first one. Upon the second reduction, the electron population considerably increases on the Ni d, F, and CO_2H (Table V). Interestingly, the overlap population of C–O^a significantly decreases upon the second one-electron reduction and becomes a negative value of −0.201, while it is rather small but positive (0.041) in $[Ni^IF(NH_3)_4(CO_2H)]^+$. This strongly supports that OH^- easily dissociates from $NiF(NH_3)_4(CO_2H)$ upon the second one-electron reduction, yielding OH^- and $[Ni^{II}F(NH_3)_4(CO)]^+$, as proposed by Sauvage et al.[6]

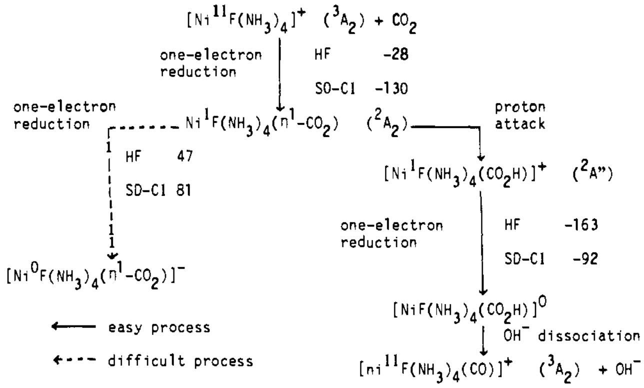

Figure 4. Schematic representation of energy change caused by reduction (kcal/mol).

Electronic State and CO Coordinate Bond of $[Ni^{II}F(NH_3)_4(CO)]^+$. In $[Ni^{II}F(NH_3)_4(CO)]^+$ which is formed from $NiF(NH_3)_4(CO_2H)$ through the OH^- dissociation, there are two possible electronic states, $^1A_1(d_{z^2}{}^2d_{xy}{}^0)$ and $^3A_2(d_{z^2}{}^1d_{xy}{}^1)$. Of these two states, the latter is calculated to be more stable than the former at both HF and SD-CI levels (Table IV). This is in accordance with the result that $NiF(NH_3)_4(CO_2H)$ is calculated to be triplet and the singlet OH^- dissociates from it.

Then, the Ni–CO distance is optimized for this electronic state with the SD-CI method, because CO dissociates from Ni with no barrier at the HF level. The optimized Ni–CO distance is rather long, 2.4 Å, and the binding energy of CO is only 10 kcal/mol at the SD-CI level. This weak CO coordination can be understood by considering a weak π back-bonding from Ni^{II} d_π to CO π*; the Ni d_π electron population decreases only by 0.012 upon CO coordination to Ni^{II}.[44] Consequently, CO dissociates easily from Ni^{II}, which suggests that the catalytic cycle of electrochemical reduction of CO_2 by $NiCl_2$(cyclam) is completed, as proposed by Sauvage et al.[6b]

Concluding Remarks

Ab initio MO/SD-CI calculations were carried out on $Ni^IF(NH_3)_4(\eta^1\text{-}CO_2)$, $[Ni^I(NH_3)_4(\eta^1\text{-}CO_2)]^+$, $[Ni^I(NH_3)_5(\eta^1\text{-}CO_2)]^+$, $[Ni^{II}F(NH_3)_4(\eta^1\text{-}CO_2)]^+$, $Ni^IF(NH_3)_4(\eta^2\text{-}CO_2)$, $[Ni^I(NH_3)_4(\eta^2\text{-}CO_2)]^+$, and $[Ni^I(NH_3)_5(\eta^2\text{-}CO_2)]^+$. These complexes are considered possible models of an intermediate in electrocatalytic reduction of CO_2 by $NiCl_2$(cyclam). $Ni^IF(NH_3)_4(\eta^1\text{-}CO_2)$ exhibits a significantly large binding energy, but $[Ni^I(NH_3)_5(\eta^1\text{-}CO_2)]^+$ exhibits a small one, while others are calculated to be unstable for CO_2 coordination. By considering the nature of the frontier orbital of the metal fragment, we can explain the reason that $Ni^IF(NH_3)_4(\eta^2\text{-}CO_2)$, $[Ni(NH_3)_4(\eta^2\text{-}CO_2)]^+$, and $[Ni(NH_3)_5(\eta^2\text{-}CO_2)]^+$ are unstable. The HOMO of $Ni^IF(NH_3)_4$ is a half-occupied d_{xy} orbital, and the next HOMO is a doubly occupied d_{z^2} orbital which extends toward CO_2. The d_{xz} and d_{yz} orbitals lie lower in energy than the d_{z^2} orbital. This favors the η^1-C coordination but disfavors the η^2-side-on coordination, because a strong charge-transfer interaction from Ni d_{z^2} to CO_2 π* stabilizes the η^1-CO_2 complex. A difference between the stable $Ni^IF(NH_3)_4(\eta^1\text{-}CO_2)$ and the other η^1-CO_2 complexes is found in the presence of an anionic F^- ligand and the +1 oxidation state of Ni. Coordination of an anion ligand pushes the d_{z^2} orbital up

---

(44) The Ni d orbital population decreases by 0.014 electron upon CO_2 coordination to $[Ni^{II}F(NH_3)_4]^+$ and by 0.012 electron upon CO coordination to $[Ni^{II}F(NH_3)_4)]^+$. Nevertheless, CO_2 coordination is significantly unstable, but CO coordination is somewhat stable. This difference between CO and CO_2 can be interpreted in terms of the coordinate bond nature of CO and CO_2. In CO_2 coordination, only Ni $d_\sigma \rightarrow CO_2$ π* charge transfer is significantly important, for CO_2 π and n_π orbitals hardly contribute to the coordinate bond because of their substantially low orbital energies. In CO coordination, on the other hand, both σ donation from the CO lone pair to Ni and π back-donation from Ni dπ to CO π* are important. Thus, the CO coordination to Ni^{II} is somewhat stable, whereas the back-bonding interaction is weak as in CO_2 coordination.

in energy, to enhance the charge transfer from Ni d_{z^2} to CO_2 π^*, and neutralizes the positive charge of Ni^I, to reduce the charge–dipole repulsion between the bending CO_2 and Ni^I. The reduction of Ni^{II} to Ni^I also destabilizes the Ni d orbitals in energy, which favors the charge transfer from Ni d_{z^2} to CO_2 π^*. These factors enable CO_2 to coordinate to $Ni^IF(NH_3)_4$ in the η^1-C coordination mode. In this stable $Ni^IF(NH_3)_4(\eta^1\text{-}CO_2)$, the HOMO consists of the Ni d_σ and deformed π^* orbital of CO_2 in which the O p_π orbital is enhanced in size and the C p_π orbital is diminished. This feature of the HOMO comes from the orbital mixing of Ni d_{z^2} and CO_2 π and π^* orbitals, and results in the considerably large electron density on O of CO_2. Consequently, the reactivity for proton attack is enhanced from viewpoints of frontier and charge controls. Proton attack yields $[Ni^IF(NH_3)_4(\eta^1\text{-}CO_2H)]^+$ which has the structure of a typical M–CO_2H complex. This species easily undergoes the second one-electron reduction, while the unprotonated species $Ni^IF(NH_3)_4(\eta^1\text{-}CO_2)$ has difficulty undergoing the second reduction. The second reduction weakens the C–OH bond very much. As a result, the OH^- anion easily dissociates from $NiF(NH_3)_4(\eta^1\text{-}CO_2H)$, yielding $[Ni^{II}F(CO)(NH_3)_4]^+$. This Ni^{II}–carbonyl complex takes a triplet $^3A_2(d_{z^2}{}^1d_{xy}{}^1)$ state. The CO binding energy of this complex is very small, 10 kcal/mol at the SD-CI level, which indicates that CO easily dissociates from Ni^{II}. All these results offer strong support to the reaction mechanism proposed by Sauvage et al.

Also, these results suggest how to improve the catalytic system of CO_2 electrochemical reduction by Ni^{II}(cyclam): (1) coexistence of such a coordinating anionic ligand as Cl^- or use of an anode adsorbing metal complex, to stabilize the $\eta^1\text{-}CO_2$ coordination, (2) use of a protic solvent, to make protonation facile, and (3) use of an appropriate buffer solution, to neutralize OH^- produced with CO (high concentration of OH^- suppresses protonation).

A Theoretical Approach to Drug Design. 3. Relative Thermodynamics of Inhibitor Binding by *E. coli* Dihydrofolate Reductase to Ethyl Derivatives of Trimethoprim Substituted at the 3′, 4′, and 5′ Positions

Joseph J. McDonald[†] **and Charles L. Brooks III***

Contribution from the Department of Chemistry, Carnegie Mellon University, Pittsburgh, Pennsylvania 15213. Received April 17, 1991

Abstract: The relative binding thermodynamics of trimethoprim [2,4-diamino-5-(3′,4′,5′-methoxybenzyl)pyrimidine] congeners to *E. coli* dihydrofolate reductase have been determined using free energy simulation methods. The thermodynamics associated with methoxy to ethyl substitutions at the 3′, 4′, and 5′ positions on the benzyl ring of trimethoprim have been calculated. The simulations have been carried out for both the binary DHFR/inhibitor and ternary DHFR/NADPH/inhibitor complexes to examine the effects of the cofactor on inhibitor binding. A model structure was computed for the *E. coli* DHFR ternary complex based upon crystallographic structures of the *E. coli* DHFR/trimethoprim and *L. casei* DHFR/NADPH/methotrexate complexes. The conformation of residues 12–25 in the modeled ternary complex, known to undergo a conformational transition upon cofactor binding, reproduces the conformation seen in a recently solved structure of the *E. coli* DHFR/NADP(+)/folate complex. In six of the seven tested congeners, the transformation from trimethoprim to ethylated derivative is preferred in the DHFR/inhibitor system over the DHFR/inhibitor/NADPH system. Further, the presence of cofactor and the conformational differences in residues 12–25 of the ternary complex have a significant effect on the magnitude of energetic and entropic components associated with the relative binding thermodynamics. The protein environment differences between the binary and ternary complexes affect the overall relative binding free energies in a complex manner which appears to be related to both the degree of inhibitor ethylation and the solvent exposure of the transformed functional groups.

Introduction

Dihydrofolate reductase catalyzes the NADPH-linked reduction of 7,8-dihydrofolate to 5,6,7,8-tetrahydrofolate. Trimethoprim, a substituted benzylpyrimidine, is a competitive inhibitor of dihydrofolate reductase with pharmacological applications to treatment of bacterial infections.[1,2] A strong positive cooperativity in the binding of trimethoprim has been noted for the *E. coli* form of dihydrofolate reductase, dependent on the presence of NADPH cofactor, which varies according to the degree of benzyl methoxy substitution.[3] This cooperativity is believed, in part, to confer the approximately 3000 times greater specificity for trimethoprim in *E. coli* dihydrofolate reductase over a mammalian form of the enzyme. In addition, a variety of close structural analogues of trimethoprim have been studied which differ at the methoxy substituents on the benzyl ring, and show antibacterial affinities which vary with the different substitutions.[4–7] The results of these antibacterial studies have been used to formulate structural and chemical requirements for effective dihydrofolate reductase ligands based on QSAR methodologies.[8,9]

The relative binding affinities of the different trimethoprim congeners are dependent on changes in the relative free energies of inhibitor binding. Differences in binding free energies of related

---

[*] Author to whom correspondence should be addressed.

[†] Current address: Monsanto Company, Department of Biological Chemistry, 700 Chesterfield Village Parkway, Chesterfield, MO 63198.

(1) Hitchings, G. H.; Roth, B. In *Enzyme Inhibitors as Drugs*; Sandler, M., Ed.; Macmillan: New York, 1980, pp 263–280.

(2) Hitchings, G. H. *Agnew. Chem., Int. Ed. Engl.* **1989**, *28*, 879.

(3) Baccanari, D. P.; Daluge, S.; King, R. W. *Biochemistry* **1975**, *21*, 5068.

(4) Roth, B.; Aig, E.; Lane, K.; Rauchkman, B. S. *J. Med. Chem.* **1980**, *23*, 535.

(5) Roth, B.; Aig, E. *J. Med. Chem.* **1987**, *30*, 1998.

(6) Roth, B.; Rauckman, B. S.; Ferone, R.; Baccanari, D. P.; Champness, J. N.; Hyde, R. M. *J. Med. Chem.* **1987**, *30*, 348.

(7) Li, R.-L.; Poe, M. *J. Med. Chem.* **1988**, *31*, 366.

(8) Dietrich, S. W.; Blaney, J. M.; Reynolds, M. A.; Jow, P. Y. C.; Hansch, C. *J. Med. Chem.* **1980**, *23*, 1205.

(9) Selassie, C. D.; Fang, Z.-X.; Li, R.-L.; Hansch, C.; Debnath, G.; Klein, T. E.; Langridge, R.; Kaufman, B. T. *J. Med. Chem.* **1989**, *32*, 1895.

0002-7863/92/1514-2062$03.00/0 © 1992 American Chemical Society